International Biodeterioration & Biodegradation 142 (2019) 83–90

Contents lists available at ScienceDirect

International Biodeterioration & Biodegradation

journal homepage: www.elsevier.com/locate/ibiod

Cloning and characterization the nicotine degradation enzymes 6-hydroxypseudooxynicotine amine oxidase and 6-hydroxy-3-succinoylpyridine hydroxylase in *Pseudomonas geniculata* N1

Weiwei Wang[a,1], Xiongyu Zhu[a,1], Xin Liu[a], Wei Wu[b], Ping Xu[a], Hongzhi Tang[a,*]

[a] State Key Laboratory of Microbial Metabolism, and School of Life Sciences & Biotechnology, Shanghai Jiao Tong University, Shanghai, 200240, People's Republic of China

[b] Befar Group Co., LTD., Binzhou, Shandong, 256619, People's Republic of China

ARTICLE INFO

Keywords:
Nicotine degradation
Pseudomonas geniculata N1
VPP pathway
6-HPON amine oxidase (HisD)
HSP monooxygenase (VD)

ABSTRACT

Microbial catabolism plays a crucial role in the removal of toxic alkaloids including nicotine from tobacco waste. *Pseudomonas geniculata* N1, an effective nicotine-degrader, possesses a variant of the pyridine and pyrrolidine (VPP) nicotine catabolic pathway. In this study, a 20-kbp gene cluster was found to contain eight nicotine-degrading genes. In comparison to *Sphingomonas melonis* TY, *Ochrobactrum* sp. SJY1, *Shinella* sp. HZN7, and *Agrobacterium tumefaciens* S33, these genes are tightly clustered in the *P. geniculata* N1 genome. The gene *hisD* encoding a 6-hydroxypseudooxynicotine (6-HPON) amine oxidase was heterologously expressed in *Pseudomonas putida* KT2440 and the recombinant strain acquired the ability to transform 6-HPON to 6-hydroxy-3-succinoylpyridine (HSP). The *vD* gene encodes a flavin-containing NADH-dependent monooxygenase, which converted HSP to 2,5-dihydroxypyridine was cloned in *E. coli* and characterized. Both genes, *hisD* and *vD*, were significantly upregulated in response to nicotine. This study expands our knowledge of the VPP nicotine catabolic pathway in bacteria.

1. Introduction

The development of the tobacco industry worldwide has increased public attention on the toxicity and remediation of waste products, including nicotine (Novotny and Slaughter, 2014). European Union regulations classified nicotine as a "toxic and hazardous waste" chemical in 1999, and the American Medical Association also provided guidelines to control the nicotine level in tobacco production (Novotny and Zhao, 1999; Henningfield et al., 1998). Research on nicotine degradation by microorganisms first began in the 1950s (Wada and Yamasaki, 1953). Microbial treatment plays an important role in the treatment of nicotine from tobacco industry waste (Civilini et al., 1997; Wang et al., 2013; Zhong et al., 2010). Microorganisms that have evolved a variety of nicotine degradation pathways include *Arthrobacter* (Brandsch, 2006), *Pseudomonas* (Tang et al., 2012a; Qiu et al., 2013), *Ochrobactrum* (Yuan et al., 2005), *Agrobacterium* (Wang et al., 2012), *Shinella* (Ma et al., 2014a), and *Aspergillus* (Meng et al., 2010). Based on identification of intermediates, two major nicotine catabolism pathways (the pyridine pathway and the pyrrolidine pathway) have been proposed in bacteria, and the molecular biology and mechanisms of these pathways have been comprehensively elucidated (Brandsch, 2006; Tang et al., 2013). Recently, a nicotine degradation pathway designated as a variant of pyridine and pyrrolidine (VPP) pathway has been reported (Yu et al., 2015a, 2015b). The molecular mechanism of nicotine degradation in the VPP pathway has been elucidated, providing a potential application to quitting smoking in the clinic (Xue et al., 2015).

Several bacteria with the ability to degrade nicotine via the variant pathway have been isolated and characterized, such as *Ochrobactrum* sp. strain SJY1 (Yu et al., 2015a, 2015b), *Agrobacterium tumefaciens* S33 (Wang et al., 2009), *Shinella* sp. strain HZN7 (Qiu et al., 2014), and *Pusillimonas* sp. strain T2 (Ma et al., 2014b). The upstream portion of the VPP pathway is congruent with the upstream part of the pyridine pathway, which is the route from nicotine to 6-hydroxypseudooxynicotine (6-HPON) through to 6-hydroxynicotine (6-HN) and 6-hydroxy-*N*-methylmyosmine (6-HMM). Meanwhile, the downstream portion of the VPP pathway is in perfect accordance with the downstream portion of the pyrrolidine pathway. In this part of the

* Corresponding author. School of Life Sciences & Biotechnology, Shanghai Jiao Tong University, Shanghai, 200240, People's Republic of China.
E-mail address: tanghongzhi@sjtu.edu.cn (H. Tang).

[1] These authors contributed equally to this work.

https://doi.org/10.1016/j.ibiod.2019.05.003
Received 26 March 2019; Received in revised form 6 May 2019; Accepted 6 May 2019

pathway, 6-hydroxy-3-succinoylpyridine (HSP) is gradually catabolized to TCA cycle through the intermediates 2,5-dihydroxypyridine (2,5-DHP). The transformation of 6-HPON to HSP, which is different from the pyridine and pyrrolidine pathways, links the upstream and downstream portions of the VPP pathway. *Pseudomonas geniculata* N1 catabolizes nicotine via the VPP pathway based on an analysis of intermediates (Liu et al., 2014). Moreover, the major molecular mechanism of the VPP pathway in *Ochrobactrum* sp. strain SJY1 has been determined, and three key enzymes were characterized in strain SJY1. In contrast, the reaction transforming 6-HPON to HSP, the crucial step connecting the upstream and downstream parts of the VPP pathway, remains unknown.

In the present study, a *vpp* gene cluster of *Pseudomonas geniculata* N1 was predicted to be responsible for nicotine degradation based on our previous work (Tang et al., 2012b). On the basis of genome sequencing of strain N1, eight genes showing relatively high identity with the reported genes involved in nicotine degradation were found in a 20-kbp DNA fragment. To our knowledge, this is the first study to describe the VPP pathway of nicotine catabolism in *Pseudomonas*. Moreover, the function of *hisD* and *vD* were identified in this study. The *hisD* gene is the core gene for the VPP pathway that connects the upstream portion of the pyridine pathway with the downstream portion of the pyrrolidine pathway. A full determination of the molecular mechanism for this reaction is vitally important for understanding the VPP pathway. In this study, we revealed the molecular mechanism of nicotine degradation in *Pseudomonas geniculata* N1 and present key information for further research into the VPP pathway.

2. Materials and methods

2.1. Reagents and media

L-Nicotine (purity, > 99%) was bought from Fluka Chemie GmbH (Switzerland). 6-HN (Yu et al., 2015b), 6-HPON (Yu et al., 2015a), and HSP (Yu et al., 2014) were prepared as previously described (Fig. S3). 2,5-DHP was bought from SynChem OHG (Kassel Corp., Kassel, Germany). FAD and NADH were bought from Shanghai Sangon Biotech (China). Nicotine medium was prepared as previously reported (Wang et al., 2004). All other reagents used in this study are commercially available.

2.2. Strains and plasmids

The strains and plasmids are shown in Table 1. *Pseudomonas geniculata* N1, isolated from tobacco leaves, were cultured at 30 °C in the nicotine medium. *Pseudomonas putida* KT2440 and *Escherichia coli* BL21 were cultured in LB medium at 30 °C and 37 °C, respectively.

2.3. Cloning and expression of the hisD and vD gene

The *hisD* and *vD* genes were amplified using primers found in Table 1 and genomic DNA of strain N1 as template. The *hisD* gene fragment was then digested by restriction enzymes *EcoRI* and *BglII* and ligated into *EcoRI-BglII* sites of pME6032 vector (Heeb et al., 2000) to form recombinant plasmid pME6032-hisD cloned in *E. coli* DH5a cells. The recombinant plasmid was sequenced and transferred into strain KT2440 (Nelson et al., 2002) via electroporation. The PCR product of *vD* gene was digested by *NdeI* and *HindIII* and ligated into pET28a vector to form recombinant plasmid pET28a-vD with a His-tagged N-terminal. The recombinant plasmid was confirmed by sequencing and transferred into *E. coli* BL21(DE3). The strains carrying the plasmid pME6032-hisD and plasmid pET28a-vD were cultured in LB medium with working concentration of 25 μg mL^{-1} tetracycline or 50 μg mL^{-1} kanamycin separately (37 °C, 180 rpm). When the bacteria reached the exponential phase (OD_{600} = 0.6–0.8), 0.5 mM (working concentration) IPTG was added to the medium. The strains were cultured for another 12 h at 20 °C and then harvested. After washing twice with 10 mM PBS, the cells were resuspended to an optical density at 600 nm (OD_{600}) of 8.0 as resting cells and 5.0 mM 6-HPON was added as the substrate in the resting cells at 30 °C. The products of the reaction, catalyzed by resting cells of *P. putida* KT2440 with pME6032-hisD (KThisD-pME), were analyzed and identified by high-pressure liquid chromatography (HPLC) and LC-MS. The function of gene *vD* in *E. coli* pET28a-vD were determined by the disappearance of HSP after 5.0 mM HSP was added in the resting cells as above. After incubation, samples were analyzed by HPLC and LC-MS.

2.4. Purification and assays of HisD protein

The *hisD* gene was cloned into shuttle plasmid pVLT33 (Lorenzoa et al., 1993; Yang et al., 2008) to generate pVLT33-*hisD*. *P. putida* KT2440 carrying pVLT33-*hisD* (*P. putida* KThisD-pVLT) was grown to exponential phase at 30 °C and induced with addition of 1 mM IPTG at 22 °C for 12 h. The harvested cells were lysed by ultrasonic treatment, centrifuged at 10,000 * g for 40 min, and the supernatant was added to a Ni-sepharose column, washed with 25 mM Tris-HCl (pH 7.0), and eluted with 25 mM Tris-HCl containing 200 mM imidazole. Imidazole in the eluted fractions was removed by ultrafiltration. After affinity chromatography, the eluted fractions were separated by ion exchange chromatography, using a column filled with Source 15Q 4.6/100 PE (GE Healthcare, Little Chalfont, United Kingdom). The reactions catalyzed by HisD were performed in 10 mM PBS of pH 7.0 containing 5 mM 6-HPON, 6-HMM and 5 μg mL^{-1} purified HisD at room temperature. The enzymatic function was identified by HPLC and LC-MS by detecting the production of HSP and 6-hydroxy-3-succinoylsemialdehyde-pyridine (HSSAP).

2.5. Purification and assays of VD

The *vD* gene was amplified with primers *vD*-F/*vD*-R, and the PCR product was cloned into plasmid pET28a to generate pET28a-*vD*. *E. coli* BL21(DE3) carrying pET28a-*vD* was grown into the exponential phase at 37 °C, and then induced with addition of 0.5 mM IPTG at 22 °C overnight. The harvested cells were lysed by ultrasonic treatment and then centrifuged at 10,000 * g, and the supernatant was added to a Ni-sepharose column and washed by the buffer as mentioned above. The imidazole in the eluted fractions was removed by ultrafiltration. Enzymatic activities were measured by spectrophotometric analysis at 25 °C and pH 8.0. Enzymatic reaction of VD was detected with the addition of enzyme (working concentration 0.0085 mg mL^{-1}), 250 μM HSP and 250 μM NADH. By measuring the decrease of NADH absorption at 340 nm, the enzyme activity of VD was determined spectrophotometrically. FAD was added to test the effects of FAD binding to the enzymes. The reaction products were determined by LC-MS.

2.6. Cofactor FAD/FMN determination of VD and HisD

Protein concentration was measured by modified Bradford protein assay kit (Sangon Biotech, Shanghai). FAD and FMN were identified and quantitatively analyzed by HPLC as described previously (Tang et al., 2011). The standard curve for FAD is shown in Fig. S2 and the standard curve for FMN is shown in Fig. S4. The protein VD solution (2.5 mg mL^{-1}, ~63 μM) and HisD (2.2 mg mL^{-1}, ~30 μM) were boiled for 5 min and then centrifuged at 12,000 rpm for 30 min to isolate the flavin cofactor.

2.7. RT-qPCR experiments

Minimal salt medium with 5 mg mL^{-1} glycerol and 1 mg mL^{-1} NH_4Cl was used in the control groups (Tang et al., 2013). Strain N1 was grown at 30 °C to mid-exponential phase in the medium in the presence and absence of nicotine, and total RNAs was extracted using an

Table 1
Strains, plasmids and primers in this study.

Strain, plasmid, or primer	Description or primer sequence	Source
Strains		
Pseudomonas geniculata N1	Nicotine-degrading strain, Gram negative	CCTCC M2011183
Pseudomonas putida		
KT2440	Metabolically versatile saprophytic soil bacterium	Nelson et al. (2002)
KT6032	KT2440 containing pME6032	This study
KTpVLT	KT2440 containing pVLT33	This study
KThisD-pME	KT2440 containing pME6032-hisD	This study
KThisD-pVLT	KT2440 containing pVLT33-hisD	This study
Escherichia coli		
DH5α	F recA1 endA1 thi-1 hsdR17 supE44 relA1 deoR(lacZYA-argF) U169 80dlacZM15	TransGen, China
BL21(DE3)	F- ompT hsdS(rB - mB -) gal dcm(DE3)	TransGen, China
Plasmids		
pME6032	Tet^r, shuttle vector	Heeb et al. (2000)
pME6032-hisD	Tet^r, pME6032 containing *hisD*	This study
pVLT33	Kan^r, expression vector in *Pseudomonas*	Lorenzoa et al., (1993); Yang et al., (2008)
pVLT33-hisD	Kan^r, pVLT33 containing *hisD*	This study
pET28a	Kan^r, expression vector	TransGen
pET28a-vD	Kan^r, pET28a containing *vD*	This study
Primers		
hisD-F	cgGAATTC atgcgcgatccccgttac	This study
hisD-R	gaAGATCT tcactcgacggacgtc	This study
hisD-tag-F	ttcacacaggaaacaGAATTCatgcgcgatccccgttacg	This study
hisD-tag-R	aaacagccAAGCTTcaatggtgatggtgatgatgctcgacggacgtcccgtagc	This study
vD-F	ggaattcCATATGgccaagcatgtgatcg	This study
vD-R	cccAAGCTTcagaagtgcgtctccatctgc	This study
hisD-RTq-F	gaggagacgatgatacac	This study
hisD-RTq-R	cgatgtacttgtcagagt	This study
vD-RTq-F	attgagggtatcgagcag	This study
vD-RTq-F	atagggcgagtaggcaac	This study

RNAprep pure bacteria kit (TianGen, China). The cDNA were then prepared using SuperScript III reverse transcriptase (Invitrogen). The primers for RT-PCR of the *hisD* and *vD* genes are shown in Table 1. The quantitative PCR was performed using the CFX96 Real-Time PCR Detection system (Bio-Rad, CA) with SYBR green Realmaster Mix (TianGen, China).

2.8. Analytical methods

6-HMM, 6-HPON, HSP, and 2,5-DHP were detected by HPLC using an Agilent eclipse XDB-C_{18} reverse-phase column (5 μm; 4.6 by 150 mm) at 25 °C and the UV detector was set at 259 nm for nicotine, 6-HMM, 6-HPON, HSP and 307 nm for 2,5-DHP. The flow rate of mobile phase was 0.5 mL min^{-1} and was composed of 85% (vol:vol) 5 mM formic acid and 15% (vol:vol) methanol. LC-MS was carried out by an Agilent 6230 time of flight (TOF)-MS with electrospray ionization (ESI) sources in the same mobile phase as HPLC. The enzyme reaction was determined by spectrum scanning using a UV2550 spectrophotometer (Shimadzu, Kyoto, Japan). By measuring the decrease of NADH absorbance at 340 nm, reaction rate was measured to obtain kinetic data. All data from enzyme reactions were obtained by three independent experiments.

2.9. Nucleotide sequence accession number

The *vpp* cluster of *Pseudomonas geniculata* N1 can be found with the GenBank accession number NZ_AJLO02000002.

3. Results

3.1. The hisD gene is responsible for biotransformation of 6-HPON to HSP

Biotransformation of 6-HPON to HSP is the core reaction in the VPP pathway. To determine the function of the *hisD* gene, the vector pME6032 harboring the *hisD* gene was heterologously expressed in *P. putida* KT2440. The reaction involved incubating the substrate of 5.0 mM 6-HPON (containing 6-HMM) with resting cells of KT6032 (KT2440 containing pME6032) and KThisD-pME (KT2440 containing pME6032-hisD). In the reaction of cells carrying only the empty pME6032 vector, there was no new product formation as determined by HPLC. In the reaction with KThisD-pME resting cells after 24 h, the substrate peak at retention time of 5.0 min decreased, while two new product peaks emerged, one at 13.7 min, which was consistent with the retention time of a standard of HSP (Fig. 1A); the other new product peak emerged at 11.8 min. The two new products were then analyzed using LC-MS. One was found to have a molecular weight of 195.0532 (m/z = 196.0604), which was identical to HSP, and the other was found to have a molecular weight of 179.0582 ((m/z = 180.0794), which was identical to 6-hydroxy-3-succinoylsemialdehyde-pyridine (HSSAP) (Fig. 1B).

3.2. The vD gene is responsible for biotransformation of HSP to 2,5-DHP

The conversion of HSP to 2,5-DHP is the first step in the downstream portion of the VPP pathway, and follows the reaction catalyzed by HisD. There is a genomic distance of 1.5-kb between *vD* and *hisD*, where a transcriptional regulator and a hypothetical protein are present, based on available annotation by RAST (http://rast.nmpdr.org/). To determine the function of the *vD* gene, the resting cell reaction of *E. coli* BL21(DE3) carrying plasmid pET28a-vD (or pET28a, a blank control) was conducted. The substrate HSP disappeared in the sample carrying the plasmid pET28a-vD, and a new peak appeared at 4.5 min (absent in the control), which was consistent with the retention time of standard 2,5-DHP (Fig. S1-A). After addition of a standard of 2,5-DHP to the sample, the peak area increased, which indicated that the product of the reaction was 2,5-DHP. The new product was analyzed using LC-MS and the determined molecular weight of 112.0395 was identical to the 2,5-DHP standard (Fig. S1-B). There were no new peaks that appeared in the control groups. The other product for the step catalyzed by VD should be succinic semialdehyde according to our previous report (Tang et al., 2011), but we did not conduct this test in the present study. These data showed that the *vD* gene was responsible for the

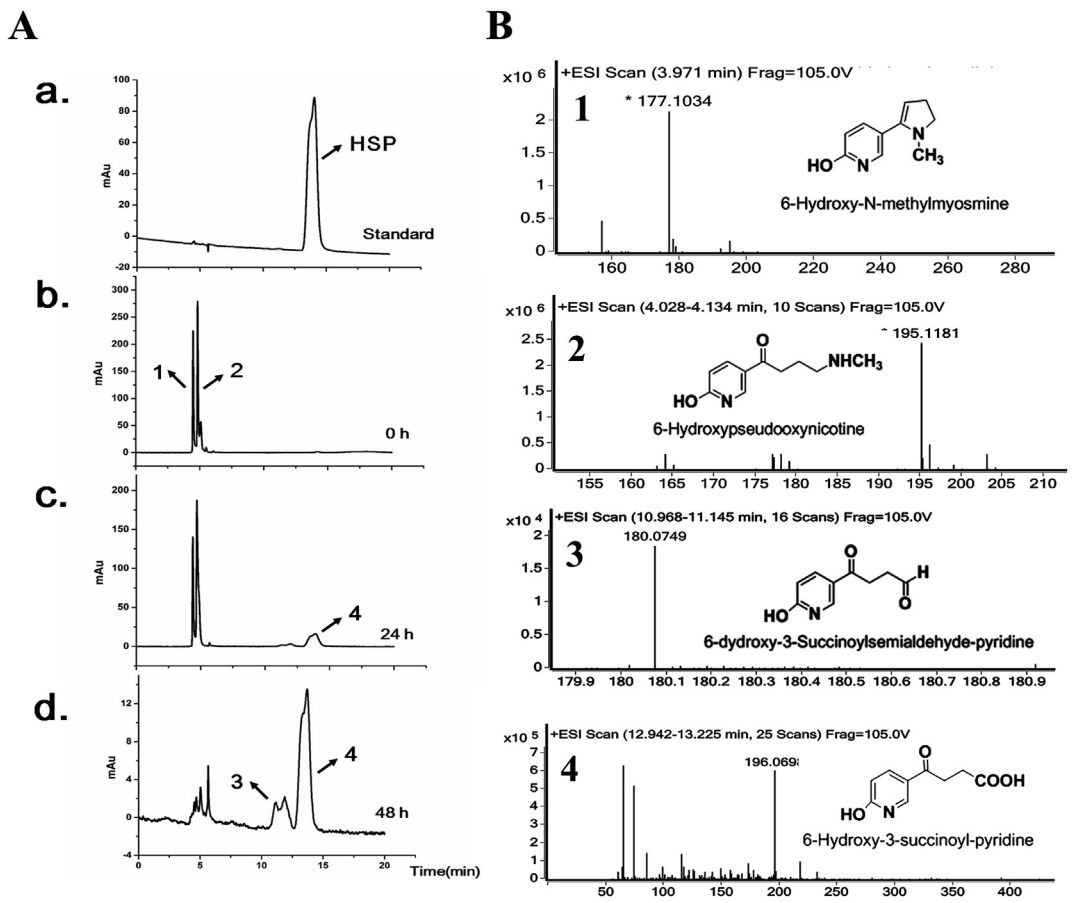

Fig. 1. The functional identification of the genes *hisD*. (A) The HPLC profile of product identification by the resting cell reaction of *P. putida* KT2440 containing plasmids pME6032-hisD using 6-hydroxypseudooxynicotine (6-HPON) containing 6-hydroxy-N-methylmyosmine (6-HMM) as the substrate. (a) Standard 6-Hydroxy-3-succinoylpyridine (HSP); (b) 6-HPON (containing 6-HMM) as the substrate at 0 h; (c) the product after resting cell reaction at 24 h; (d) the product after resting cell reaction at 48 h . (B)The LC-MS analysis of the product after resting cells reaction of KThisD-pME. 1–2, mass spectra of the substrate 6-HPON and 6-HMM; 3–4, mass spectra of the product 6-Hydroxy-3-succinoylsemialdehyde-pyridine (HSSAP) and HSP.

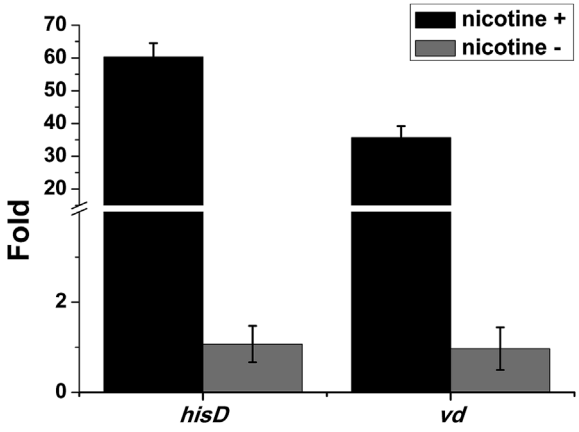

Fig. 2. Quantitative RT-PCR analysis of the genes *hisD* and *vD*. The relative expression levels of the *hisD* and *vD* genes were measured using RNA extracted from *Pseudomonas geniculata* N1 grown in the presence (+) or absence (−) of nicotine. All data were normalized to the 16S rRNA and are expressed as fold change relative to the expression level in cells.

conversion of HSP to 2,5-DHP in the VPP pathway (Fig. 3).

3.3. The hisD and vD genes are upregulated in the presence of nicotine

Pseudomonas geniculata N1 is a nicotine-degrading bacterium that utilizes nicotine as its sole carbon and nitrogen source. Genes associated with nicotine metabolism are usually upregulated in the presence of nicotine (Tang et al., 2013). To test this notion, the transcription levels of the *vD* and *hisD* genes in the presence of various concentrations of nicotine were studied by quantitative PCR. The results revealed that the transcription levels of *hisD* and *vD* were significantly increased under the influence of nicotine as compared to these genes in the absence of nicotine (fold changes of 57 and 32, respectively), suggesting that *hisD* and *vD* genes expression are involved in nicotine degradation (Fig. 2). The results of RT-qPCR showed that the *hisD* and *vD* genes are up-regulated during nicotine degradation in strain N1.

3.4. HisD is a 6-HPON amine oxidase and catalyzes transformation of 6-HPON to HSP

Plasmid pVLT33 is an effective expression vector in *Pseudomonas* species (Lorenzoa et al., 1993; Yang et al., 2008). His-tagged HisD was heterologously expressed in *P. putida* KT2440 cells, and isolated on a Ni-Sepharose column (Fig. 4A) and further purified by ion exchange chromatography (Fig. 4B). The purified HisD was confirmed by SDS-PAGE (Fig. S4). HisD protein was incubated with 6-HPON, and its resulting activity was extremely low (Fig. S5). After the enzymatic reaction progressed for 72 h, two products HSSAP and HSP were identified using LC-MS analysis (Fig. S6). Compound HSP was the main product of the reaction, and found that the substrates 6-HPON and 6-HMM were not stable (Fig. S5-A). The color of the control assay turned black over time, but there was no color change in the assay containing purified HisD.

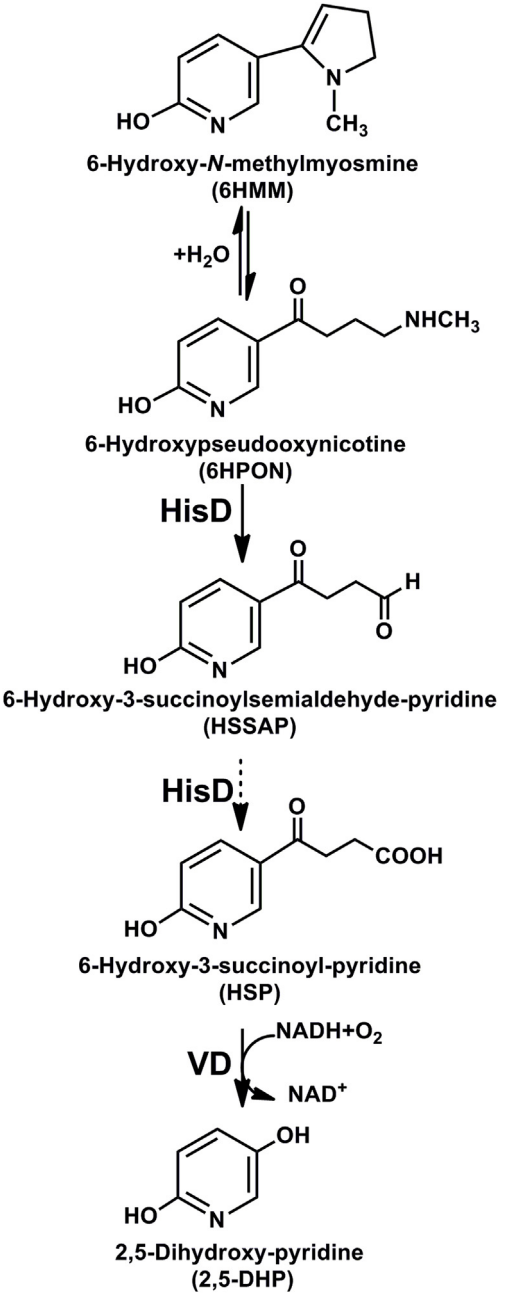

Fig. 3. The proposed reactions from 6-HMM to 2,5-dihydroxy-pyridine (2,5-DHP): 6-HMM is spontaneously hydrolyzed to form 6-HPON. 6-HPON is oxidized by the protein encoded by *hisD* to form HSSAP and HSP. HSP is oxidized by the protein encoded by *vD* to produce 2,5-dihydroxypyridine (2,5-DHP).

Conserved domain analysis showed that HisD harbors one FMN and one [4Fe–4S] cluster. Purified HisD is a yellow brown protein with characteristic absorption peaks of flavin and an iron-sulfur cluster shown in Fig. 4C, indicating that the protein may belong to the iron-sulfur protein family (You et al., 2007; Li et al., 2015). The cofactor of HisD was found to have an identical retention time (~17 min) and its spectrum curve (Fig. S2-C & D) was identical to an FMN standard. Furthermore, the FMN concentration in the purified HisD solution (30 μM) was 26 μM, suggesting that one HisD protein harbors one FMN cofactor.

3.5. VD is an HSP 3-monooxygenase

The transformation from HSP to 2,5-DHP can also be catalyzed by

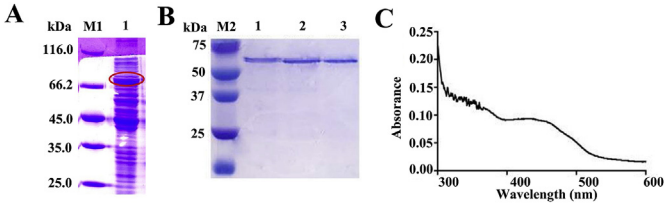

Fig. 4. Purification and UV-visible absorption spectrum of HisD protein from *P. putida* KT2440 containing plasmids pVLT33-hisD. (A) HisD purified by HisTrap HP column in 50 mM sodium phosphate buffer (pH 7.0). Collecting this sample for further purification. (B) Using the sample above to separated HisD by ion exchange chromatography. HisD was purified in the condition of 0.4 mol–0.5 mol NaCl (pH 7.0). (C) Spectrum scanning of HisD protein. The arrow indicates the characteristic absorption peak in 420 nm.

HspB from *P. putida* S16 (Tang et al., 2011), which shows 46.3% amino acid sequence identity with the VD protein. VD was heterologously expressed in *E. coli* and purified (Fig. 5A and B), and it was shown that it can convert HSP to 2,5-DHP in the presence of NADH, revealing NADH-dependent HSP 3-monooxygenase activity. Enzyme kinetics showed that the apparent K_m for NADH (at 250 μM HSP) was 75.62 μM (Fig. 5C) and the apparent K_m for HSP (at 250 μM NADH) was 35.94 μM (Fig. 5D). These values were less than the values of HspB, indicating that the VD protein had stronger affinity for the substrates. The optimal temperature of VD was nearly 20 °C (Fig. 5E) and temperatures above 35 °C easily disrupted stability of the protein (Fig. 5F). The optimal pH of VD was found to be ~8.5 (Fig. 5G), and Cd^{2+} and Zn^{2+} strongly inhibited its activity (Fig. 5H). Based on the sequence analysis, VD contained an FAD-binding domain described in our previous work (Tang et al., 2011; Yu et al., 2015a). HPLC results showed that the cofactor isolated from VD protein solution was FAD (retention time ~23 min). The spectrum curve of FAD boiled from VD on HPLC is shown in Fig. S2-A & C.

4. Discussion

In this study, the functions of two genes, *hisD* and *vD*, were investigated, and the protein HisD was found to be responsible for the transformation from 6-HPON to HSSAP and HSP. The reaction, which links the pyridine pathway and pyrrolidine pathway, is the core reaction in the VPP pathway (Fig. 3). Protein HisD was found to be a 6-HPON amine oxidase, which was 82% identical to Pno in the *Agrobacterium tumefaciens* strain S33. HSSAP was the product of 6-hydroxypseudooxynicotine oxidation catalyzed by the Pno enzyme (Li et al., 2015). However, in this study both HSSAP and HSP were found in the reaction products of 6-HPON oxidation catalyzed by HisD or resting cells of KThisD-pME. The amino acid sequence of HisD suggested a histamine dehydrogenase (HD) FMN-binding domain and a trimethylamine dehydrogenase (TMADH) domain. The conserved domain suggested that HisD is an iron-sulfur flavoprotein, containing a 4Fe–4S cluster and an FMN cofactor. The characteristic peaks of HisD detected using the UV 2550 spectrophotometer were congruent with the prediction of the conserved domain and confirmed that HisD belonged to the iron-sulfur flavoprotein family. The HisD protein did not show a capacity for 6-HPON oxidation during heterologous expression in *E. coli* harboring the ISC cluster (Nakamura et al., 1999; Raulfs et al., 2008), suggesting that 4Fe–4S is not the sole cofactor in the HisD enzyme and that other unknown cofactors are also necessary for the enzymatic activity.

HisD is annotated as a histamine dehydrogenase on the RAST annotation server. Based on alignment with histamine dehydrogenases from NCBI (Fig. 6), HisD was found to be similar to the histamine dehydrogenase in *Ochrobactrum* SJY1, which is also a VPP pathway-carrying microorganism, and indicated that the protein in SJY1 was likely to catalyze the same reaction in strain SJY1. Histamine dehydrogenase

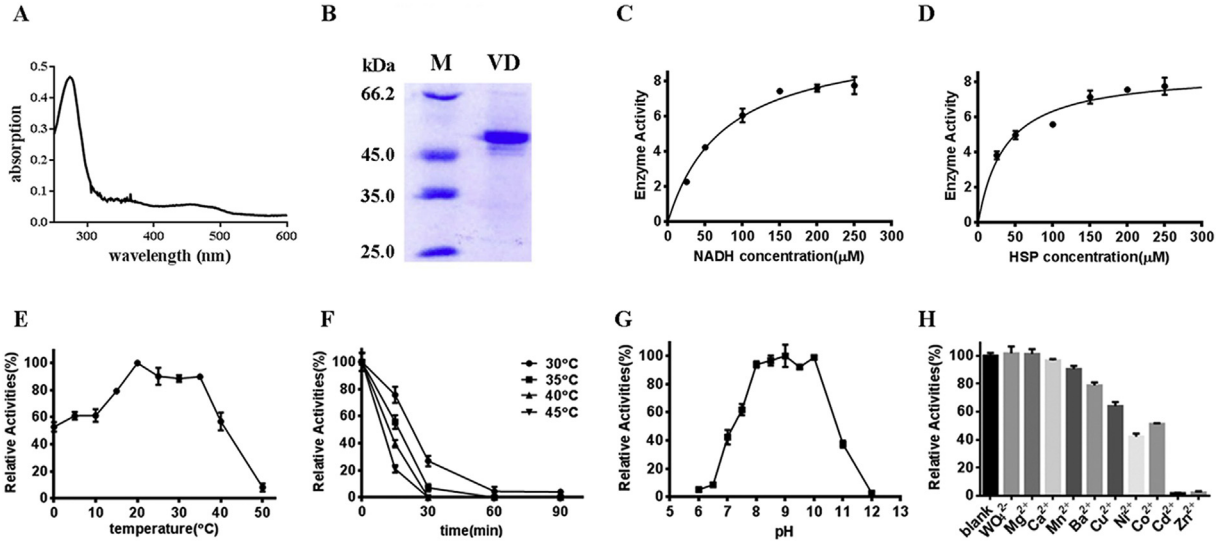

Fig. 5. Characterization of VD protein. (A) The spectrum scanning of VD; (B) SDS-PAGE of purified VD; (C) Kinetic studies of VD, fitted to the Michaelis-Menten curve for HSP (at 250 μM NADH); (D) Kinetic studies of VD, fitted to the Michaelis-Menten curve for NADH (at 250 μM HSP); (E) The effect of reaction temperature for VD; (F) Stability of heat for VD; (G) pH optimization of VD; (H) The effect of metal ion for VD.

catalyzes the oxidative deamination of histamine to imidazole acetaldehyde, suggesting that proteins in the histamine dehydrogenase family contain a covalently bound cofactor as a quinone-like compound (Fujieda et al., 2004; Datta et al., 2001). In *Pseudomonas putida*, histamine dehydrogenase is covalently bound to cysteine tryptophylquinone as the redox active prosthetic group (Satoh et al., 2002; Roduit et al., 1997). According to phylogeny, HisD has the same conserved domain as some typical histamine dehydrogenases and significant identity (43.6%) with histamine dehydrogenase in *Ralstonia solanacearum* FQY_4, but HisD did not show any detectable activity toward histamine in the present study. HSP hydroxylase from strain N1 catalyzed the conversion of HSP to 2,5-DHP in the presence of NADH; 2,5-DHP is a valuable precursor for the synthesis of prescription drugs and insecticides (Wang et al., 2005). In the VPP pathway, HSP hydroxylation immediately follows the reaction catalyzed by HisD. The VD protein, which catalyzed the transformation of HSP to 2,5-DHP, contained the conserved motifs for FAD that shared some amino acid sequence identity (46.3%) with VppD from strain SJY1.

According to the gene sequence alignment, similar gene clusters related to the VPP pathway of nicotine catabolism were found in strains of *Pseudomonas geniculata* N1, *Sphingomonas melonis* TY (Wang et al., 2017), *Ochrobactrum* sp. SJY1, *Agrobacterium tumefaciens* S33, and *Shinella* sp. HZN7 (Fig. 7A). According to comparisons of the *vpp* cluster in the strain N1 and other strains utilizing nicotine via the VPP pathway, the nicotine-degrading genes were tightly clustered in strain N1's chromosomal genome (Table 2). There was a 15- to 20-kb gap in the *vpp* cluster in strains SJY1, S33, and HZN7, while the genes in strain N1 and strain TY were arranged together. There was a similar gap between the gene encoding HSP hydroxylase and the gene encoding 6-HPON oxidase, and two hypothetical genes of similar length were found in the gap. This is the first report of a nicotine-degrading gene cluster that functions via the VPP pathway in *Pseudomonas*. According to clustered genetic organization and high similarity of amino acid sequence between N1 and TY, these two strains appear to have evolved from horizontal gene transfer although they belong to different genus. Amino acid sequence alignments showed that the two proteins VD and HisD in N1 share 56% and 82% similarity, respectively, with the two proteins in SJY1. Gene annotation showed that there was one gene, between *hisD* and *vD*, that encoded a TetR family regulator, and it may have a regulatory function in 6-HPON oxidation or HSP hydroxylation. The genes

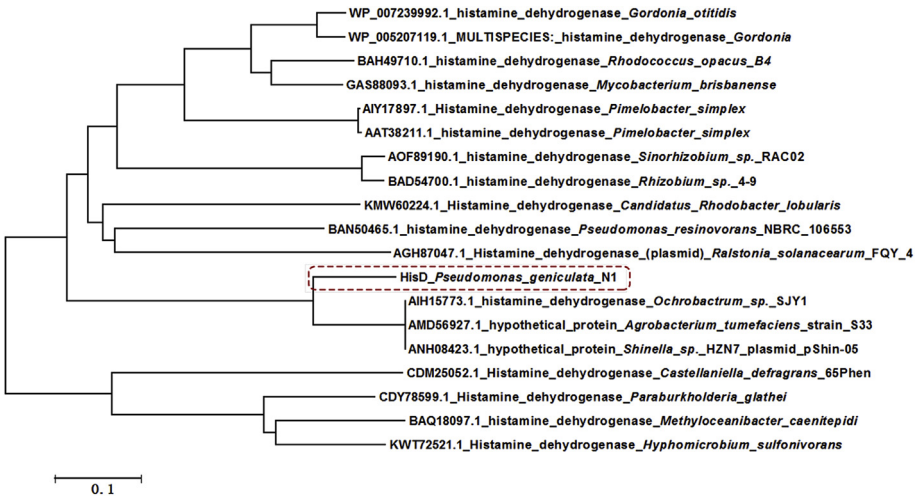

Fig. 6. Multiple alignment and phylogenetic analysis of HisD and related histamine dehydrogenase from NCBI. The GenBank accession number for each protein is shown.

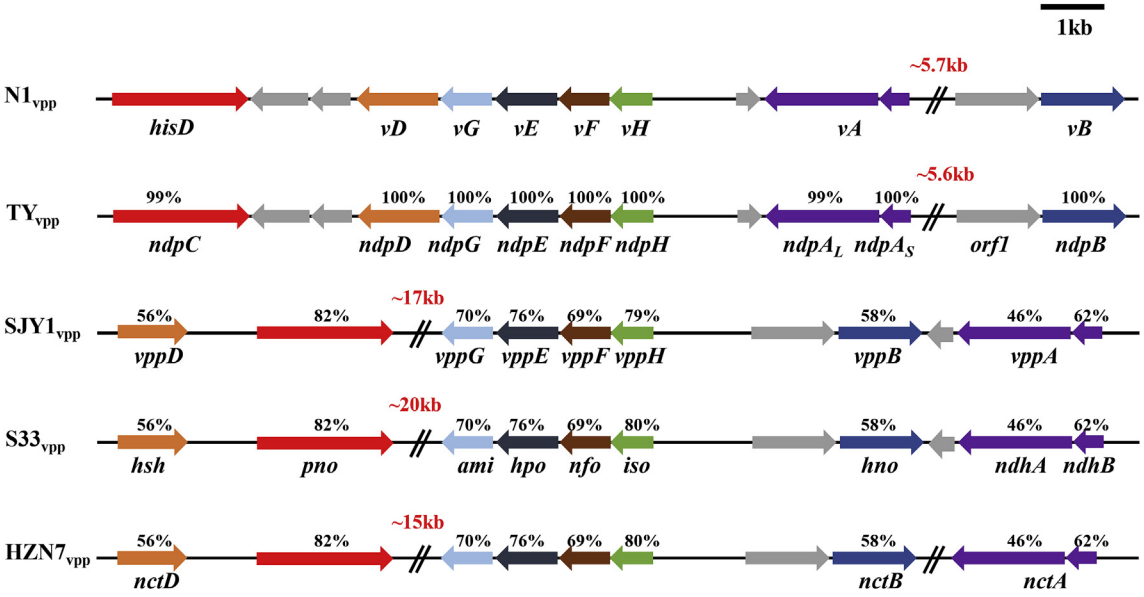

Fig. 7. The analysis of *vpp* gene cluster in *Pseudomonas geniculata* N1. (A) The *vpp* cluster in *Pseudomonas geniculata* N1 (GenBank accession number NZ_AJLO02000002), *Sphingomonas melonis* TY (GenBank accession number LQCK02000019.1), *Ochrobactrum* sp. SJY1 (GenBank accession number KM065745), A. *tumefaciens* S33 (GenBank accession number CP014259) and *Shinella* sp. HZN7 (GenBank accession number CP015741). The arrows indicate the size and direction of the transcription of each gene, and genes with the same fill color are homolog enzymes. *vA* in N1, *ndpAL* and *ndpAS* in TY, *vppA* in SJY1, *ndhA* and *ndhB* in S33, *nctA* in HZN7, encoding nicotine hydroxylase; *vB* in N1, *ndpB* in TY, *vppB* in SJY1, *hno* in S33, *nctB* in HZN7, encoding 6-hydroxy-nicotine oxidase; *hisD* in N1, *ndpC* in TY, *pno* in S33, encoding 6-hydroxypseudooxynicotine oxidase; vD in N1, ndpD in TY, vppD in SJY1, hsh in S33, nctD in HZN7, encoding HSP monooxygenase; *vE* in N1, *ndpE* in TY, *vppE* in SJY1, *hpo* in S33, encoding 2,5-DHP dioxygenase; *vF* in N1, *ndpF* in TY, *vppF* in SJY1, *nfo* in S33, encoding N-formylmaleamic acid deformylase; *vG* in N1, *ndpG* in TY, *vppG* in SJY1, *ami* in S33, encoding maleamate amidase; *vH* in N1, *ndpH* in TY, *vppH* in SJY1, *iso* in S33, encoding maleate isomerase. The nucleotide sequence identities are shown above the genes.

in N1 (*vA*, *vB*, *vE*, *vF*, *vG*, and *vH*) have similar amino acid sequences (46%/62%, 58%, 70%, 76%, 69%, and 79% respectively) to the genes in strain SJY1 (*vppA*, *vppB*, *vppE*, *vppF*, *vppG*, and *vppH*, respectively), thus pointing to a similar function in the VPP pathway. Our previous work reported that strain N1 was able to degrade nicotine into myosmine, cotinine and 2,6-dihydroxypseudooxynicotine (Liu et al., 2014), which were not present in the reported VPP pathway. However, related genes, including the gene encoding ketone dehydrogenase (KDH), which could convert 6-hydroxypseudooxynicotine to 2,6-dihydroxypseudooxynicotine, were not found on the N1 chromosomal genome. This indicates that, in addition to the VPP gene cluster, the N1 strain may have other nicotine metabolic gene clusters.

5. Conclusion

In summary, we identified two enzymes (HisD and VD) that catalyzed key reactions in the VPP pathway. The hisD gene encoded an enzyme, 6-HPON amine oxidase, which converted 6-HPON to HSP in the VPP pathway. The vD gene, which encoded an HSP hydroxylase, was found to convert HSP to 2,5-DHP. Further research into enzyme HisD is still needed for a complete understanding of this pathway. Meanwhile, the complete gene cluster related to the VPP pathway in N1 chromosome genome was identified and comparison of the *vpp* cluster among different species may provide more information about the horizontal transfer of nicotine-degrading genes, Ultimately, this comparison will enable researchers to gain insights into the molecular mechanism of the VPP pathway.

Table 2
The *vpp* gene cluster identified in the N1 genome.

location	start	stop	strand	function	length	name
N1vpp_4240_6258	4240	6258	+	Histamine dehydrogenase	2019	***hisD***
N1vpp_6999_6274	6999	6274	–	Transcriptional regulator, TetR family	726	
N1vpp_7531_7034	7531	7034	–	hypothetical protein	498	
N1vpp_9144_7981	9144	7981	–	Monooxygenase, FAD-binding	1164	***vD***
N1vpp_9815_9195	9815	9195	–	N-carbamoylsarcosine amidase	621	***vG***
N1vpp_10809_9802	10809	9802	–	Leucyl aminopeptidase	1008	***vE***
N1vpp_11668_10847	11668	10847	–	Hydrolase, alpha/beta fold family functionally coupled to Phosphoribulokinase	822	***vF***
N1vpp_12420_11668	12420	11668	–	Maleate cis-trans isomerase	753	***vH***
N1vpp_13495_13878	13495	13878	+	hypothetical protein	384	
N1vpp_16313_14082	16313	14082	–	Isoquinoline 1-oxidoreductase beta subunit	2232	***vA***
N1vpp_16743_16321	16743	16321	–	Isoquinoline 1-oxidoreductase alpha subunit	423	***vA***
N1vpp_20154_17830	20154	17830	–	Outer membrane receptor proteins, mostly Fe transport	2325	
N1vpp_20663_20809	20663	20809	+	hypothetical protein	147	
N1vpp_20812_22041	20812	22041	+	Permeases of the major facilitator superfamily	1230	
N1vpp_22038_22487	22038	22487	+	Translation initiation inhibitor	450	
N1vpp_22484_23884	22484	23884	+	Aldehyde dehydrogenase	1401	
N1vpp_23917_25401	23917	25401	+	Amine oxidase [flavin-containing] A	1485	***vB***

Acknowledgements

This study was supported by grants from the Science and Technology Commission of Shanghai Municipality (17JC1403300), China; the 'Shuguang Program' (17SG09) co-supported by the Shanghai Education Development Foundation and Shanghai Municipal Education Commission, China; the National Natural Science Foundation of China (31270154 and 31422004), China.

Appendix A. Supplementary data

Supplementary data to this article can be found online at https://doi.org/10.1016/j.ibiod.2019.05.003.

Conflicts of interest

The authors declare no competing interests.

References

Brandsch, R., 2006. Microbiology and biochemistry of nicotine degradation. Appl. Microbiol. Biotechnol. 69, 493–498. https://doi.org/10.1007/s00253-005-0226-0.

Civilini, M., Domenis, C., Sebastianutto, N., de Berfoldi, M., 1997. Nicotine decontamination of tobacco agro-industrial waste and its degradation by micro-organisms. Waste Manag. Res. 15, 349–358. https://doi.org/10.1177/0734242X9701500403.

Datta, S., Mori, Y., Takagi, K., Kawaguchi, K., Chen, Z.W., Okajima, T., Okajima, T., Kuroda, S., Ikeda, T., Kano, K., Tanizawa, K., Mathews, F.S., 2001. Structure of a quinohemoprotein amine dehydrogenase with an uncommon redox cofactor and highly unusual crosslinking. Proc. Natl. Acad. Sci. U.S.A. 98, 14268–14273. https://doi.org/10.1073/pnas.241429098.

Fujieda, N., Satoh, A., Tsuse, N., Kano, K., Ikeda, T., 2004. 6-S-Cysteinyl flavin mononucleotide-containing histamine dehydrogenase from *Nocardioides* simplex: molecular cloning, sequencing, overexpression, and characterization of redox centers of enzyme. Biochemistry 43, 10800–10808. https://doi.org/10.1021/bi049061q.

Heeb, S., Itoh, Y., Nishijyo, T., Schnider, U., Keel, C., Wade, J., Walsh, U., O'Gara, F., Haas, D., 2000. Small, stable shuttle vectors based on the minimal pVS1 replicon for use in gram-negative, plant-associated bacteria. Mol. Plant Microbe Interact. 13, 232–237. https://doi.org/10.1094/MPMI.2000.13.2.232.

Henningfield, J.E., Benowitz, N.L., Slade, J., Houston, T.P., Davis, R.M., Deitchman, S.D., 1998. Reducing the addictiveness of cigarettes. Tobac. Contr. 7, 281–293. https://doi.org/10.1136/tc.7.3.281.

Li, H., Xie, K., Yu, W., Hu, L., Huang, H., Xie, H., Wang, S., 2015. Nicotine dehydrogenase complexed with 6-hydroxypseudooxynicotine oxidase involved in the hybrid nicotine-degrading pathway in *Agrobacterium tumefaciens* S33. Appl. Environ. Microbiol. 82, 1745–1755. https://doi.org/10.1128/AEM.03909-15.

Liu, Y., Wang, L., Huang, K., Wang, W., Nie, X., Jiang, Y., Li, P., Liu, S., Xu, P., Tang, H., 2014. Physiological and biochemical characterization of a novel nicotine-degrading bacterium *Pseudomonas geniculata* N1. PLoS One 9, e84399. https://doi.org/10.1371/journal.pone.0084399.

Lorenzoa, V., Eltisb, L., Kesslerb, B., Timmisb, K.N., 1993. Analysis of *Pseudomonas* gene products using *lacP/Ptrp-lac* plasmids and transposons that confer conditional phenotypes. Gene 123, 17–24. https://doi.org/10.1016/0378-1119(93)90533-9.

Ma, Y., Wei, Y., Qiu, J., Wen, R., Hong, J., Liu, W., 2014a. Isolation, transposon mutagenesis, and characterization of the novel nicotinedegrading strain *Sh*inella sp. HZN7. Appl. Microbiol. Biotechnol. 98, 2625–2636. https://doi.org/10.1007/s00253-013-5207-0.

Ma, Y., Wen, R., Qiu, J., Hong, J., Liu, M., Zhang, D., 2014b. Biodegradation of nicotine by a novel strain Pusillimonas. Res. Microbiol. 166, 67–71. https://doi.org/10.1016/j.resmic.2014.12.009.

Meng, X.J., Lu, L.L., Gu, G.F., Xiao, M., 2010. A novel pathway for nicotine degradation by *Aspergillus oryzae* 112822 isolated from tobacco leaves. Res. Microbiol. 161, 626–633. https://doi.org/10.1016/j.resmic.2010.05.017.

Nakamura, M., Saeki, K., Takahashi, Y., 1999. Hyperproduction of recombinant ferredoxins in *Escherichia* coli by coexpression of the OKFl-ORF2-iscS-iscU-iscA-hscB-hscA-fdx-ORF3 Gene Cluster. J. Biochem. 126, 10–18. https://doi.org/10.1093/oxfordjournals.jbchem.a022409.

Nelson, K.E., Weinel, C., Paulsen, I.T., Dodson, R.J., Hilbert, H., dos Santos, V.M., Fouts, D.E., Gill, S.R., Pop, M., Holmes, M., Brinkac, L., Beanan, M., DeBoy, R.T., Daugherty, S., Kolonay, J., Madupu, R., Nelson, W., White, O., Peterson, J., Khouri, H., Hance, I., Chris Lee, P., Holtzapple, E., Scanlan, D., Tran, K., Moazzez, A., Utterback, T., Rizzo, M., Lee, K., Kosack, D., Moestl, D., Wedler, H., Lauber, J., Stjepandic, D., Hoheisel, J., Straetz, M., Heim, S., Kiewitz, C., Eisen, J.A., Timmis, K.N., Düsterhöft, A., Tümmler, B., Fraser, C.M., 2002. Complete genome sequence and comparative analysis of the metabolically versatile P*seudomonas putida K*T2440. Environ. Microbiol. 4, 799–808. https://doi.org/10.1046/j.1462-2920.2002.00366.x.

Novotny, T.E., Zhao, F., 1999. Consumption and production waste: another externality of tobacco use. Tobac. Contr. 8, 75–80. https://doi.org/10.1136/tc.8.1.18.

Novotny, T.E., Slaughter, E., 2014. Tobacco product waste: an environmental approach to reduce tobacco consumption. Curr. Environ. Health Rep. 1, 208–216. https://doi.org/10.1007/s40572-014-0016-x.

Qiu, J.G., Ma, Y., Zhang, J., Wen, Y.Z., Liu, W.P., 2013. Cloning of a novel nicotine oxidase gene from *Pseudomonas* sp. strain HZN6 whose product nonenantioselectively degrades nicotine to pseudooxynicotine. Appl. Environ. Microbiol. 79, 2164–2171. https://doi.org/10.1128/AEM.03824-12.

Qiu, J.G., Wei, Y., Ma, Y., Wen, R.T., Wen, Y.Z., Liu, W.P., 2014. A novel (*S*)-6-Hydroxynicotine oxidase gene from *Shinella* sp. strain HZN7. Appl. Environ. Microbiol. 80, 5552–5560. https://doi.org/10.1128/AEM.01312-14.

Raulfs, E.C., O'Carroll, I.P., Dos Santos, P.C., Unciuleac, M.C., Dean, D.R., 2008. In vivo iron-sulfur cluster formation. Proc. Natl. Acad. Sci. U.S.A. 105 (25), 8591–8596. https://doi.org/10.1073/pnas.0803173105.

Roduit, J.P., Wellig, A., Kiener, A., 1997. Renewable functionalized pyridines derived from microbial metabolites of the alkaloid (S)-nicotine. Heterocycles 45, 1687–1702.

Satoh, A., Kim, J.K., Miyahara, I., Devreese, B., Vandenberghe, I., Hacisalihoglu, A., Okajima, T., Kurodas, S., Adachi, O., Duine, J.A., Beeumen, J.V., Tanizawa, K., Hirotsu, K., 2002. Crystal structure of quinohemoprotein amine dehydrogenase from *Pseudomonas putida*. J. Biol. Chem. 277, 2830–2834. https://doi.org/10.1074/jbc.M109090200.

Tang, H.Z., Yao, Y.X., Zhang, D.K., Meng, X.Z., Wang, L.J., Yu, H., Ma, L., Xu, P., 2011. A novel NADH-dependent and FAD-containing hydroxylase is crucial for nicotine degradation by *Pseudomonas putida*. J. Biol. Chem. 286 (45), 39179–39187. https://doi.org/10.1074/jbc.M111.283929.

Tang, H.Z., Yao, Y.X., Wang, L.J., Yu, H., Ren, Y.L., Wu, G., Xu, P., 2012a. Genomic analysis of *Pseudomonas putida*: genes in a genome island are crucial for nicotine degradation. Sci. Rep. 2, 377. https://doi.org/10.1038/srep00377.

Tang, H.Z., Yu, H., Tai, C., Huang, K.M., Liu, Y.H., Wang, L.J., Yao, Y.X., Wu, G., Xu, P., 2012b. Genome sequence of a novel nicotine-degrading strain, *Pseudomonas geniculata* N1. J. Bacteriol. 194 (14), 3553. https://doi.org/10.1128/JB.00625-12.

Tang, H.Z., Wang, L.J., Wang, W.W., Yu, H., Zhang, K.Z., Yao, Y.X., Xu, P., 2013. Systematic unraveling of the unsolved pathway of nicotine degradation in *Pseudomonas*. PLoS Genet. 9, e1003923. https://doi.org/10.1371/journal.pgen.1003923.

Wada, E., Yamasaki, Y., 1953. Mechanism of microbial degradation of nicotine. Science 117 (3033), 152. https://doi.org/10.1126/science.117.3033.152.

Wang, S.N., Xu, P., Tang, H.Z., Meng, J., Liu, X.L., Huang, J., Chen, H., Du, Y., Blankespoor, H.D., 2004. Biodegradation and detoxification of nicotine in tobacco solid waste by a *Pseudomonas* sp. Biotechnol. Lett. 26, 1493–1496. https://doi.org/10.1023/B:BILE.0000044450.16235.65.

Wang, S.N., Xu, P., Tang, H.Z., Meng, J., Liu, X.L., Ma, C.Q., 2005. "Green" route to 6-hydroxy-3-succinoyl-pyridine from (S)-nicotine of tobacco waste by whole cells of a *Pseudomonas* sp. Environ. Sci. Technol. 39, 6877–6880. https://doi.org/10.1021/es0500759.

Wang, S.N., Liu, Z., Xu, P., 2009. Biodegradation of nicotine by a newly isolated *Agrobacterium* sp. strain S33. J. Appl. Microbiol. 107, 838–847. https://doi.org/10.1111/j.1365-2672.2009.04259.x.

Wang, S.N., Huang, H.Y., Xie, K.B., Xu, P., 2012. Identification of nicotine biotransformation intermediates by *Agrobacterium tumefaciens* strain S33 suggests a novel nicotine degradation pathway. Appl. Microbiol. Biotechnol. 95, 1567–1578. https://doi.org/10.1007/s00253-012-4007-2.

Wang, J.H., He, H.Z., Wang, M.Z., Wang, S., Zhang, J., Wei, W., Xu, H., Lv, Z., Shen, D., 2013. Bioaugmentation of activated sludge with *Acinetobacter* sp. TW enhances nicotine degradation in a synthetic tobacco wastewater treatment system. Bioresour. Technol. 142, 445–453. https://doi.org/10.1016/j.biortech.2013.05.067.

Wang, H.X., Zhi, X.Y., Qiu, J.G., Shi, L.X., Lu, Z.M., 2017. Characterization of a novel nicotine degradation gene cluster ndp in *Sphingomonas melonis* TY and its evolution analysis. Front. Microbiol. 8, 337. https://doi.org/10.3389/fmicb.2017.00337.

Xue, S., Schlosburg, J.E., Janda, K.D., 2015. A new strategy for smoking cessation: characterization of a bacterial enzyme for the degradation of nicotine. J. Am. Chem. Soc. 137 (32), 10136–10139. https://doi.org/10.1021/jacs.5b06605.

Yang, C., Zhao, Q., Liu, Z., Li, Q., Qiao, C., Mulchandani, A., Chen, W., 2008. Cell surface display of functional macromolecule fusions on *Escherichia coli* for development of an auto fluorescent whole-cell biocatalyst. Environ. Sci. Technol. 42, 6105–6110. https://doi.org/10.1021/es800441t.

You, D., Wang, L., Yao, F., Zhou, X., Deng, Z., 2007. A novel DNA modification by sulfur: DnaA is a NifS-like cysteine desulfurase capable of assembling DndC as an iron-sulfur cluster protein in *Streptomyces lividans*. Biochemistry 46, 6126–6133. https://doi.org/10.1021/bi602615k.

Yu, H., Tang, H.Z., Xu, P., 2014. Green strategy from waste to value-added-chemical production: efficient biosynthesis of 6-hydroxy-3-succinoyl-pyridine by an engineered biocatalyst. Sci. Rep. 4, 5397. https://doi.org/10.1038/srep05397.

Yu, H., Tang, H.Z., Zhu, X.Y., Li, Y.Y., Xu, P., 2015a. Molecular mechanism of nicotine degradation by a newly isolated strain, *Ochrobactrum* sp. Strain SJY1. Appl. Environ. Microbiol. 81, 272–281. https://doi.org/10.1128/AEM.02265-14.

Yu, H., Tang, H.Z., Li, Y.Y., Xu, P., 2015b. Molybdenum-containing nicotine hydroxylase genes in a nicotine degradation pathway that is a variant of the pyridine and pyrrolidine pathways. Appl. Environ. Microbiol. 81, 8330–8338. https://doi.org/10.1128/AEM.02253-15.

Yuan, Y.J., Yuan, Y.J., Lu, Z.X., Wu, N., Huang, L.J., Lü, F.X., Bie, X.M., 2005. Isolation and preliminary characterization of a novel nicotine-degrading bacterium, Ochrobactrum intermedium DN2. Int. Biodeterior. Biodegrad. 56, 45–50. https://doi.org/10.1016/j.ibiod.2005.04.002.

Zhong, W.H., Zhu, C.J., Shu, M., Sun, K.D., Zhao, L., Wang, C., Ye, Z., Chen, J., 2010. Degradation of nicotine in tobacco waste extract by newly isolated *Pseudomo*nas sp. ZUTSKD. Bioresour. Technol. 101, 6935–6941. https://doi.org/10.1016/j.biortech.2010.03.142.